Developmental Biology 338 (2010) 148–157

Contents lists available at ScienceDirect

Developmental Biology

journal homepage: www.elsevier.com/developmentalbiology

Analysis of *hoxa11* and *hoxa13* expression during patternless limb regeneration in *Xenopus*

Shiro Ohgo, Akari Itoh, Makoto Suzuki, Akira Satoh, Hitoshi Yokoyama, Koji Tamura *

Department of Developmental Biology and Neurosciences, Graduate School of Life Sciences, Tohoku University, Aobayama Aoba-ku, Sendai 980-8578, Japan

ARTICLE INFO

Article history:
Received for publication 9 July 2009
Revised 19 November 2009
Accepted 20 November 2009
Available online 1 December 2009

Keywords:
Xenopus laevis
Limb regeneration
Proximal-distal axis
hoxa11
hoxa13

ABSTRACT

During limb regeneration, anuran tadpoles and urodele amphibians generate pattern-organizing, multipotent, mesenchymal blastema cells, which give rise to a replica of the lost limb including patterning in three dimensions. To facilitate the regeneration of nonregenerative limbs in other vertebrates, it is important to elucidate the molecular differences between blastema cells that can regenerate the pattern of limbs and those that cannot. In *Xenopus* froglet (soon after metamorphosis), an amputated limb generates blastema cells that do not produce proper patterning, resulting in a patternless regenerate, a spike, regardless of the amputation level. We found that re-expression of *hoxa11* and *hoxa13* in the froglet blastema is initiated although the subsequent proximal–distal patterning, including separation of the *hoxa11* and *hoxa13* expression domains, is disrupted. We also observed an absence of *EphA4* gene expression in the froglet blastema and a failure of position-dependent cell sorting, which correlated with the altered *hoxa11* and *hoxa13* expression. Quantitative analysis of *hoxa11* and *hoxa13* expression revealed that *hoxa13* transcript levels were reduced in the froglet blastema compared with the tadpole blastema. Moreover, the expression of *sox9*, an important regulator of chondrogenic differentiation, was detected earlier in patternless blastemas than in tadpole blastemas. These results suggest that appropriate spatial, temporal, and quantitative gene expression is necessary for pattern regeneration by blastema cells.

Introduction

Urodele amphibians, including newts and salamanders, can perfectly regenerate limbs that have been amputated at any point during their lives. On the other hand, the anuran amphibian *Xenopus laevis* shows a developmental change in its ability to regenerate limbs. Although *Xenopus* tadpoles can regenerate limb buds after amputation, this ability gradually declines as metamorphosis progresses. The froglet can regenerate only spike-like cartilaginous structures that lack proper patterning (Dent, 1962; reviewed by Suzuki et al., 2006; Yokoyama, 2008). Thus, it is possible to use *Xenopus* to compare regeneration-competent and regeneration-incompetent limbs in the same species. Moreover, elucidation of why regeneration fails in metamorphosed anuran amphibians as compared with regeneration in anuran tadpoles and urodele amphibians may provide a foundation for achieving organ regeneration in regeneration-incompetent vertebrates.

The development of a three-dimensional limb structure relies on pattern formation along three axes: the anterior–posterior (AP), dorsal–ventral (DV) and proximal–distal (PD) axes (reviewed by Capdevila and Izpisua Belmonte, 2001). During limb regeneration in urodeles and in *Xenopus* tadpoles, the expression profiles of pattern formation regulators along the three axes are similar to those observed in limb development. These regulators include shh for the AP axis (Endo et al., 1997; Imokawa and Yoshizato, 1997; Torok et al., 1999), lmx-1 for the DV axis (Matsuda et al., 2001), and hoxa13 for the PD axis (Endo et al., 2000; Christen et al., 2003; Satoh et al., 2006), are similar to those observed during limb development. The formation of patternless regenerates in the *Xenopus* froglet is thought to be associated with a failure to reactivate *shh* expression for AP axis patterning (Endo et al., 2000; Yakushiji et al., 2007). However, the relationship of pattern regulators to the formation of the other axes in regeneration is largely unknown. In the PD axis of the *Xenopus* froglet limb, only the expression of *hoxa13* has been examined during regeneration. The results suggested that positional information along the PD axis is normal and that PD patterning is initiated in the froglet blastema (Endo et al., 2000). The full explanation appears more complex because the froglet limb regenerate, the spike, is a "patternless" regenerate that does not have segments/joints along the PD axis. Furthermore, the spike shows similar morphology regardless of the amputation level. Thus, further studies are required to determine why *hoxa13* re-expression in the blastema fails to direct pattern formation, resulting in patternless regenerates independent of the level of amputation.

HoxA transcription factors are thought to be involved in PD patterning during limb development. *hoxa13* and *hoxa11* show a

* Corresponding author. Fax: +81 22 795 3489.
E-mail address: tam@biology.tohoku.ac.jp (K. Tamura).

0012-1606/$ – see front matter © 2009 Elsevier Inc. All rights reserved.
doi:10.1016/j.ydbio.2009.11.026

nested pattern of expression during early limb development in amniote embryos; *hoxa13* expression is initiated and restricted more distally within the *hoxa11* expression domain. Thereafter, each expression domain is separated along the PD axis, with the *hoxa11* positive cells forming the prospective zeugopod region, whereas the *hoxa13* expressing cells comprise the autopod (Yokouchi et al., 1991; Nelson et al., 1996; Sato et al., 2007; Tabin and Wolpert, 2007; Tamura et al., 2008; Tamura et al., in press). Additionally, the *Hox* genes are thought to regulate the surface properties of the cells. Cell sorting assays have shown that developing limb bud cells along the PD axis have specific cell adhesion properties (Ide et al., 1994; Tamura et al., 1997; Yajima et al., 1999; Wada et al., 2003), which are regulated by *HoxA* genes (Yokouchi et al., 1995; Stadler et al., 2001). During limb regeneration in urodeles, *hoxa9* and *hoxa13*, members of the *HoxA* gene cluster, are activated with an overlapping expression pattern as in the developing limb bud (Gardiner et al., 1995). Although the relationships between *HoxA* genes and the cell surface properties during limb regeneration have not been elucidated, it is thought that blastema cells along the PD axis have different cell surface properties. When a donor blastema from a given position along the PD axis is grafted to the dorsal surface of a more proximal host blastema-stump junction, the donor blastema regenerates only those structures distal to its PD plane—e.g., when a wrist blastema is grafted to a mid-thigh blastema-stump junction, only the hand is regenerated from the graft, while the host blastema produces the entire hindlimb and carries or displaces the grafted regenerate to its appropriate limb level as the hindlimb forms (Crawford and Stocum, 1988). It has been suggested that position-specific cell surface properties regulate this phenomenon. When a blastema derived from a proximal amputation and a blastema derived from a distal amputation were joined together and cultured, the proximal blastema surrounded the distal blastema (Nardi and Stocum, 1983), indicating the presence of position-dependent differential cell adhesiveness with the more distal blastema showing stronger cell adhesion (Steinberg, 1970).

Misexpression of *hoxa13* has been known to lead to suppression of zeugopod formation (Yokouchi et al., 1995), suggesting that *Hox* genes display “posterior prevalence” during limb development as has been observed during vertebrate body formation (Iimura and Pourquie, 2007). To investigate the relationships between *HoxA* gene expression and PD patterning during *X. laevis* froglet limb regeneration, we have examined the expression profiles of *hoxa13* and *hoxa11* in detail. Posterior prevalence requires a level of *Hox* gene transcripts that is sufficient to repress 3′ *Hox* genes. We therefore also investigated the mRNA levels of *hoxa13* and *hoxa11* in tadpole and froglet blastemas. Furthermore, we performed cell sorting assays using blastemas at different levels along the PD axis, in order to examine the surface property of blastema cells. The expression domains of *hoxa11* and *hoxa13* never separated, and the expression level of *hoxa13* in the froglet blastema was insufficient. Moreover, proper sorting along the PD axis did not occur. These findings suggest that re-expression of *hoxa11* and *hoxa13* during spike formation does not give rise to the subsequent cellular events that are required for PD axis formation, resulting in altered morphogenesis along the PD axis.

Materials and methods

Animals

X. laevis adults and froglets were obtained from domestic animal venders. Fertilized eggs were obtained after natural mating between adult males and females stimulated with injections of 500 units of human chorionic gonadotropin (ASKA Pharmaceutical Co.). The fertilized eggs were then grown in our laboratory until they reached appropriate stages (Nieuwkoop and Faber, 1956). Tadpoles and froglets were kept at 24 °C in dechlorinated water. Limb buds and adult limbs were amputated after *Xenopus* tadpoles and froglets were anesthetized with 1:5,000 ethyl-3-aminobenzoate (Tokyo Chemical Industry) dissolved in Holtfreter's solution. Tadpole limb buds were amputated with a surgical blade (FUTABA) at the presumptive ankle or knee using a previously published fate map (Tschumi, 1957). The tadpoles were then raised for 3–7 days until fixation. We used forelimbs for analyses of froglet limb regeneration (Suzuki et al., 2006) because hindlimbs are essential for swimming and hindlimb amputation often results in drowning or exsanguination (unpublished observations). Froglet forelimbs and hindlimbs both regenerate the same spike-like structure (Robinson and Allenby, 1974; Endo et al., 2000). Froglet forelimbs were amputated with ophthalmic scissors (Nisshin EM) at the wrist or elbow after which the froglets were raised for 7–14 days.

In situ hybridization

A partial cDNA encoding *Xenopus EphA4* was amplified in a RT-PCR performed with mRNA extracted from stage 53 *Xenopus* limb buds (forward primer: 5′-CCATTGCAGCCGATGAGAGCTTC-3′; reverse primer: 5′-GTGCAGGGCATTGAAGCTGGG-3′). The PCR product was cloned into the pCRII TOPO vector (Invitrogen, La Jolla, CA) and sequenced. To synthesize an antisense RNA probe, the *EphA4* plasmid was linearized with *Not*I and transcribed with SP6 RNA polymerase (Ambion). DIG-labeled antisense RNA probes for *hoxa11*, *hoxa13*, and *sox9* were prepared as described previously (Endo et al., 2000; Yokoyama et al., 2002; Satoh et al., 2005b). *In situ* hybridizations were performed according to the method described by Yoshida et al. (1996) with minor modifications. Briefly, tissues were fixed with MEMFA (0.1 M MOPS at pH 7.4, 2 mM EGTA, 1 mM MgSO4, and 3.7% formaldehyde), embedded in Tissue-Tek O.C.T compound (Sakura), and sectioned at 10 μm in a cryostat (Leica). Proteinase K (Invitrogen) treatment was performed at 3.75 μg/ml (for tadpole blastemas) or at 5 μg/ml (for froglet blastemas) for 7 min. The sections were hybridized overnight at 58 °C and washed at 55 °C with washing buffer as described by Yoshida et al. (1996). Anti-DIG Fab fragments conjugated with alkaline phosphatase (Roche) were diluted 1:2,000 in 0.125% Blocking Reagent/TBST and applied to the washed sections overnight at 4 °C. The colorimetric reaction was performed for 3 to 10 days using 5-bromo-4-chloro-3-indolylphophate (Wako) and nitroblue tetrazolium chloride (Wako) as substrates. The sections were refixed with 4% paraformaldehyde/PBS and mounted in glycerol.

Real-time RT-PCR

Total RNA was prepared using an RNeasy mini kit according to the manufacturer's protocol (Qiagen). Total RNA was prepared from tadpole and froglet blastemas while excluding stump tissues as much as possible. cDNA was prepared using SuperScript III (Invitrogen) following the manufacturer's protocol. Two microliters of the cDNA reaction was used for real-time PCRs, which contained the fluorescent dye SYBR Green to monitor DNA synthesis (SYBR Premix Ex taq, Takara Bio.) and primers specific for *Xenopus hoxa11* (forward primer, 5′-CTTCAAGTTCGGAGACGTG-3′; reverse primer, 5′-GTATTTGGTA-TACGGGCACCT-3′), *hoxa13* (forward primer, 5′-CACGAGCCTT-TACTGCCTAT-3′; reverse primer, 5′-TCTGTACGAGCTGCTGTCT-3′), *sox9* (forward primer, 5′-GCAATTTTCAAGGCCCTACAG-3′; reverse primer, 5′-GCCTACCATTCTCTTGCAGTG-3′), and *ribosomal L8* (forward primer, 5′-GTGGTGTGGCTATGAATCCT-3′; reverse primer, 5′-ACGAG-CAGCAATAAGACCAACT-3′). These primers were designed to include intronic sequences to avoid amplifying genomic DNA. PCRs were carried out using the Light Cycler system (Roche) and the following cycling protocol: a 95 °C denaturation step for 10 s followed by 40 cycles of denaturation at 95 °C (5 s), and annealing and extension at 60 °C (20 s). The fluorescent product was detected at the end of a

72 °C extension period. Gene expression was normalized to that of *ribosomal L8*, because *ribosomal L8* mRNA levels remain relatively constant during development (Shi and Liang, 1994). The PCR products were subjected to a melting curve analysis, and the data were analyzed and quantified using Light Cycler software. The results are shown as values relative to the expression levels observed in tadpole blastemas 7 days post amputation (dpa) as standard samples. On standard samples of each figure, the values of the ratio were fixed as 1.0.

Cell culture

Preparation of single cell suspensions was performed using the method described by Yokoyama et al. (1998). Limb buds at stage 53 were divided into three regions of equal length along the PD axis (proximal, intermediate, and distal), and the proximal and distal regions were used for the experiments (see Fig. 5A). Stage 53 limb buds and froglet limbs were amputated at each level described above. Blastemas were isolated from each limb bud and limb. Proximal blastemas (amputated at the knee or elbow level) were also divided into three regions of equal length along the PD axis, and only the proximal and distal portions were used for the experiments (see Figs. 5B and C). Mesenchymal cells from the froglet blastema were isolated by removing the epidermis. Each sample was treated with 0.2% trypsin and 0.2% collagenase in Holtfreter's solution for 2 hours to loosen the connections between the cells, and the solution was replaced with 70% DMEM supplemented with 10% fetal calf serum. To obtain single cell suspensions, mesodermal tissues were dissociated by gentle pipetting. The resultant cell suspensions were filtered through a cell strainer (Falcon) to remove tissue debris and small cell clusters (e.g., ectodermal cells).

The cells in the suspensions were counted using a hemocytometer (TATAI). Cell suspensions that had been labeled with a PKH2 fluorescence staining kit (ZYNAXIS Cell Science) were mixed with the same number of unlabeled cells and placed in a small area of a culture dish with the aid of a stainless column. The culture dish was incubated overnight at 25 °C. Thereafter, the column was removed and 4% paraformaldehyde was added to fix the sample. After fixation, the cells were washed with PBS, and DAPI (final concentration, 0.5 μg/ml) was added to stain the cell nuclei.

Results

hoxa11 and *hoxa13* expression during hindlimb development

Because *hoxa11* and *hoxa13* show characteristic expression patterns along the PD axis in chick and mouse limb buds, spatiotemporal changes in *hoxa11* and *hoxa13* expression are good indicators of PD pattern formation (Yokouchi et al., 1991; Nelson et al., 1996; Yashiro et al., 2004). We first investigated *hoxa11* and *hoxa13* expression in developing *Xenopus* hindlimb buds. In the cone-shaped, stage 50 limb bud, *hoxa11* was expressed broadly in the distal limb bud mesenchyme (Fig. 1A), whereas the expression of *hoxa13* was restricted to the most distal mesenchyme (Fig. 1B), resulting in a nested expression pattern. Subsequently, in the stage 52 limb bud, the gene expression domains were completely separated along the PD axis. *hoxa11* was expressed in the subdistal region (Fig. 1C) and *hoxa13* was expressed in the most distal region (Fig. 1D). These observations are consistent with results from previous studies that partially examined the expression patterns of these genes using whole-mount preparations (Blanco et al., 1998; Endo et al., 2000; Lombardo and Slack, 2001). Furthermore, the expression shift from a nested pattern to a separated pattern agrees with observations in chick and mouse limb buds, suggesting that the developmental changes in *hoxa11* and *hoxa13* expression are highly conserved in tetrapod limb buds.

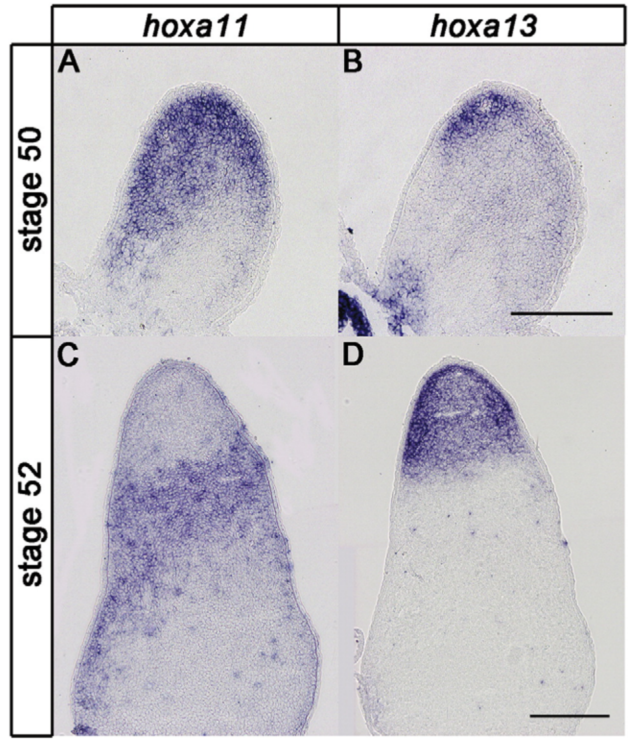

Fig. 1. *hoxa11* and *hoxa13* expressions in tadpole limb buds. (A) *hoxa11* expression in a stage 50 limb bud. *hoxa11* expression was observed broadly in the distal half of limb bud mesenchyme. (B) *hoxa13* expression in a stage 50 limb bud. Its expression was observed in the distal region. (C) *hoxa11* expression in a stage 52 limb bud. *hoxa11* was expressed in the presumptive zeugopod region. (D) *hoxa13* expression in a stage 52 limb bud. *hoxa13* was expressed in the presumptive autopod region. Distal is to the top in all figures. Scale bar = 400 μm.

hoxa11 and *hoxa13* expression in the tadpole blastema

Because *hoxa11* and *hoxa13* are good markers of PD pattern formation in *Xenopus* limbs, we next examined the expression of these *HoxA* genes during limb regeneration. We observed the temporal and spatial expression patterns of these *HoxA* cluster genes in regenerating limb buds that had been amputated at stage 53, a period at which the limb buds can regenerate a complete pattern along the PD axis (Dent, 1962; Muneoka et al., 1986). In blastema 3 dpa, *hoxa11* and *hoxa13* showed overlapping expression domains in the distal blastema at both the ankle and knee levels (Figs. 2A–D). In particular, the expression domain of *hoxa11* was broader than that of *hoxa13* in blastemas at the knee level (Figs. 2C, D). The nested expression pattern was similar to that in the distal region of early-stage developing limb buds. Strikingly, blastemas that formed at the ankle level (i.e., only the autopod region was removed) expressed *hoxa11* (Fig. 2A), although the expression of *hoxa11* had disappeared in the autopod region at this stage (see Fig. 1C). Subsequently, the changes in the expression patterns of *hoxa11* and *hoxa13* recapitulated those observed during the normal developmental process (Figs. 2E–L). In blastemas at the ankle level, the expression of *hoxa11* gradually disappeared (Fig. 2E) and was barely detectable in 7 dpa blastemas (Fig. 2I). On the other hand, the expression of *hoxa13* was observed in the entire blastema (Fig. 2J). In blastemas at the knee level, *hoxa11* expression disappeared from the distal region and remained in the proximal region (Fig. 2G), whereas the *hoxa13* expression domain was shifted distally (Fig. 2H). At 7 dpa, these expression domains were separated (Figs. 2K, L). These observations indicate that in the tadpole, which is regeneration-competent, the expression patterns of *hoxa11* and *hoxa13* seem to mirror those observed during limb development. It is interesting that ankle level amputation resulted in the maintenance of *hoxa11* expression

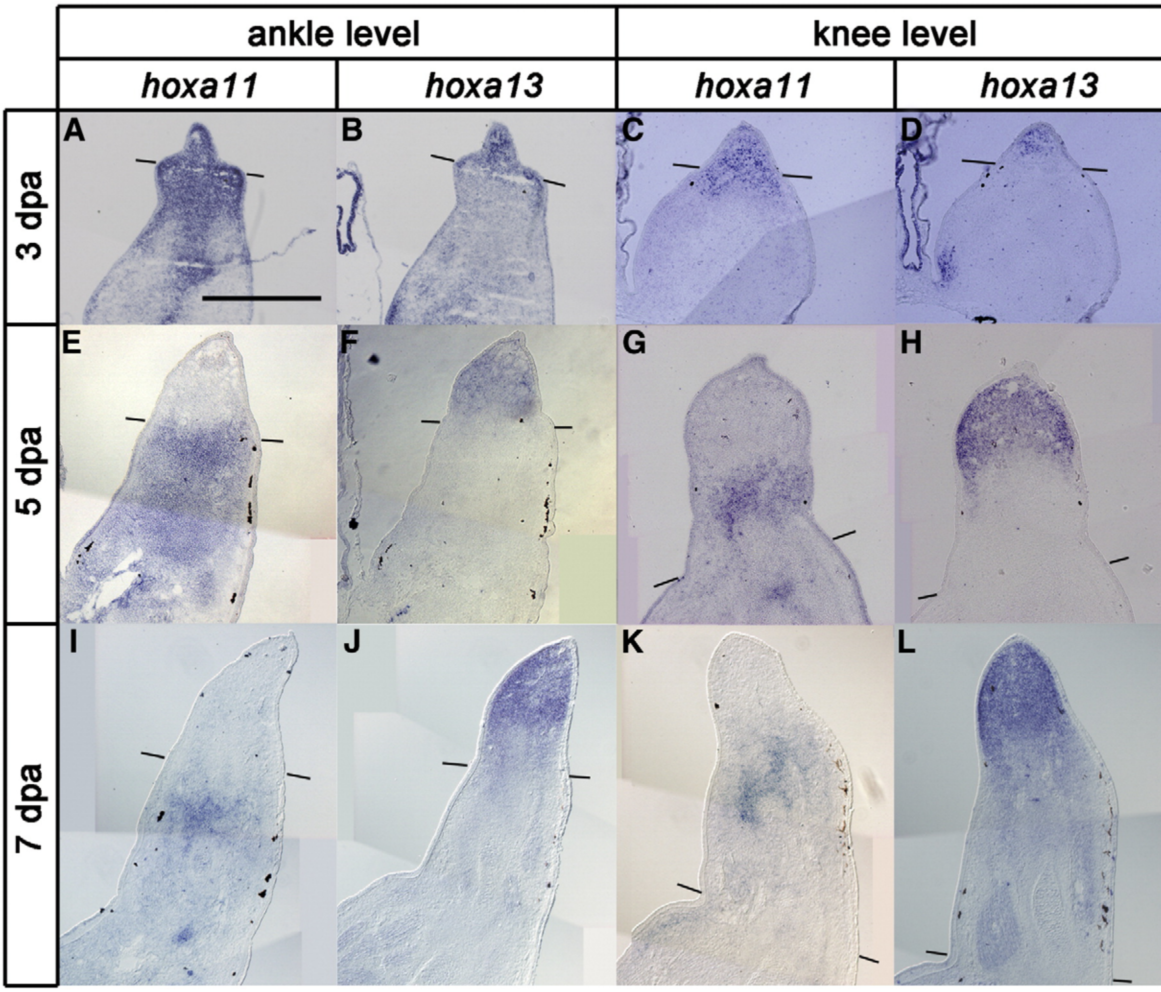

Fig. 2. *hoxa11* and *hoxa13* expressions in tadpole blastemas. Blastemas were derived from amputations at the ankle level (A, B, E, F, I and J) or at the knee level (C, D, G, H, K and L). (A, C) *hoxa11* expression in 3 days post amputation (dpa) blastema. (B, D) *hoxa13* expression in 3 dpa blastema. (E, G) *hoxa11* expression in 5 dpa blastema. (F, H) *hoxa13* expression in 5 dpa blastema. (I, K) *hoxa11* expression in 7 dpa blastema. (J, L) *hoxa13* expression in 7 dpa blastema. Note that expression patterns of *hoxa11* and *hoxa13* during tadpole limb regeneration were similar to those of a developing limb bud (Fig. 1). Lines indicate the estimated amputation planes. Distal is to the top in all figures. Scale bar = 400 μm.

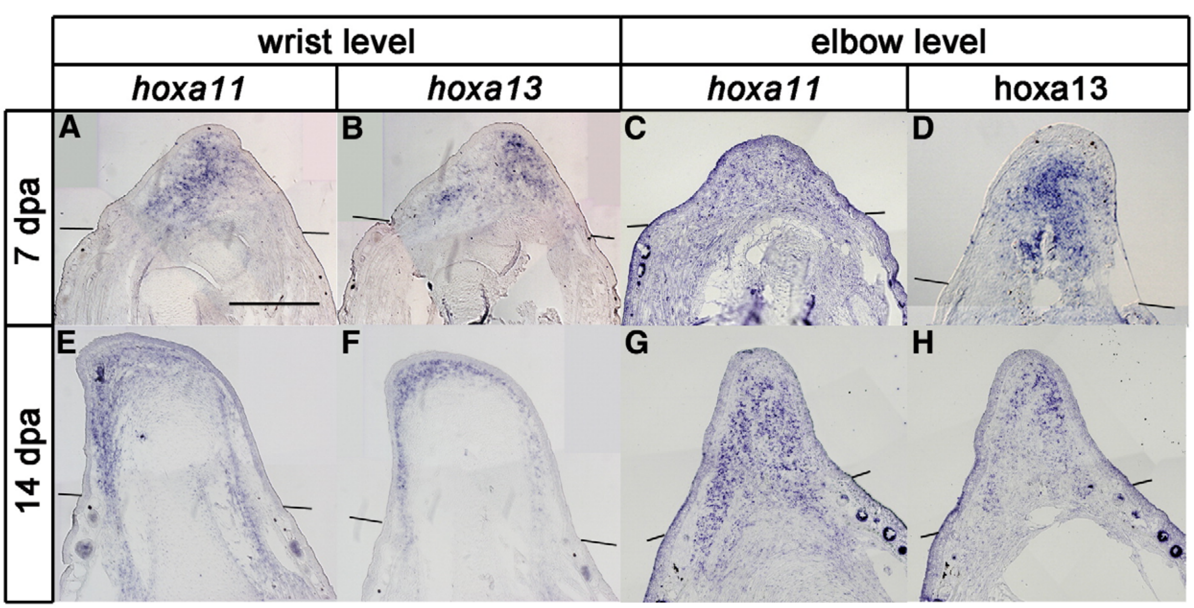

Fig. 3. *hoxa11* and *hoxa13* expressions in froglet blastemas. Blastemas were derived from amputation at the wrist level (A, B, E and F) or at the elbow level (C, D, G and H). (A, C) *hoxa11* expression in 7 days post amputation (dpa) blastema. (B, D) *hoxa13* expression in 7 dpa blastema. (E, G) *hoxa11* expression in 14 dpa blastema. (F, H) *hoxa13* expression in 14 dpa blastema. Note that *hoxa11* and *hoxa13* were reexpressed in the froglet blastema, but expression domains were never separated. Lines indicate the estimated amputation planes. Distal is to the top in all figures. Scale bar = 400 μm.

followed by its downregulation even though *hoxa11* gene expression itself is not necessary for the formation of the autopod region (Davis et al., 1995).

hoxa11 and hoxa13 expression in the froglet blastema

As mentioned above, an amputated limb of a froglet regenerates a hypomorphic spike (Dent, 1962) that lacks joints along the PD axis (Satoh et al., 2005b). We hypothesized that the froglet blastema does not display positional information along the PD axis. To assess this hypothesis, we investigated the expression patterns of *hoxa11* and *hoxa13* in the froglet forelimb blastema. *hoxa11* and *hoxa13* were expressed broadly in 7 dpa blastemas at both the wrist and elbow levels (Figs. 3A–D). The overlapping expression pattern was similar to that in tadpole 3 dpa blastemas (see Figs. 2A–D). In 14 dpa blastemas, expression of *hoxa13* was observed in the distal region (Figs. 3F, H). The expression of not only *hoxa13* but also *hoxa11* was observed distally, however, and the two expression domains were never separated along the PD axis (Figs. 3E–H). These observations suggest that positional information was disrupted in the froglet blastema, which consequently fails to form a normal PD axis.

Cartilage formation during limb regeneration

Our observations suggested a failure of PD axis formation, although it was possible that the results were merely due to slow changes in *Hox* gene expression and PD axis formation. Thus, we hypothesized that the timing between pattern determination and chondrogenesis may be altered during froglet limb regeneration. To test this hypothesis, we analyzed the expression of *sox9* as an early marker gene of chondrogenesis. In 3 dpa ankle level blastemas *sox9* was examined in the area where hoxa11 and hoxa13 overlap (Figs. 2A, B). *sox9* was expressed exclusively in the limb region proximal to the amputation plane (stump), but was absent from the blastema (Fig. 4A). Subsequently, at 5 dpa, low levels of *sox9* expression were observed in the proximal region, whereas transcripts were still not detected in the distal region of the blastema (Fig. 4B). At this stage, the expression domains of *hoxa11* and *hoxa13* began to separate (Fig. 2E, F). Finally, at 7 dpa, *sox9* expression was detected in a broad area in the central blastema (Fig. 4C). These observations suggest that during tadpole limb regeneration chondrogenesis begins after pattern determination (i.e., after the expression domains of *hoxa11* and *hoxa13* separate). On the other hand, in 7 dpa blastemas from froglets, *sox9* was expressed in the blastema prematurely (Fig. 4D), although the expression domains of *hoxa11* and *hoxa13* still overlapped at this time point (Fig. 3A, B). The expression domain of *sox9* expanded as regeneration progressed; in 14 dpa froglet blastemas, *sox9* was expressed in a broad region in the blastema (Fig. 4E). These observations were supported by the results from a quantitative analysis (Fig. 7). Taken together, the data suggest that patterning along the PD axis does not proceed normally in the froglet blastema, which may result from an early onset of cartilage differentiation.

Differences in the cell affinity properties of tadpole and froglet blastemas

Cell sorting assays showed that chick limb bud cells along the PD axis have position-dependent cell surface properties (Ide et al., 1994; Wada and Ide, 1994; Ide et al., 1998). Thus, when limb bud cells from different positions along the PD axis are mixed, the cells will aggregate with other cells derived from the same position. In contrast,

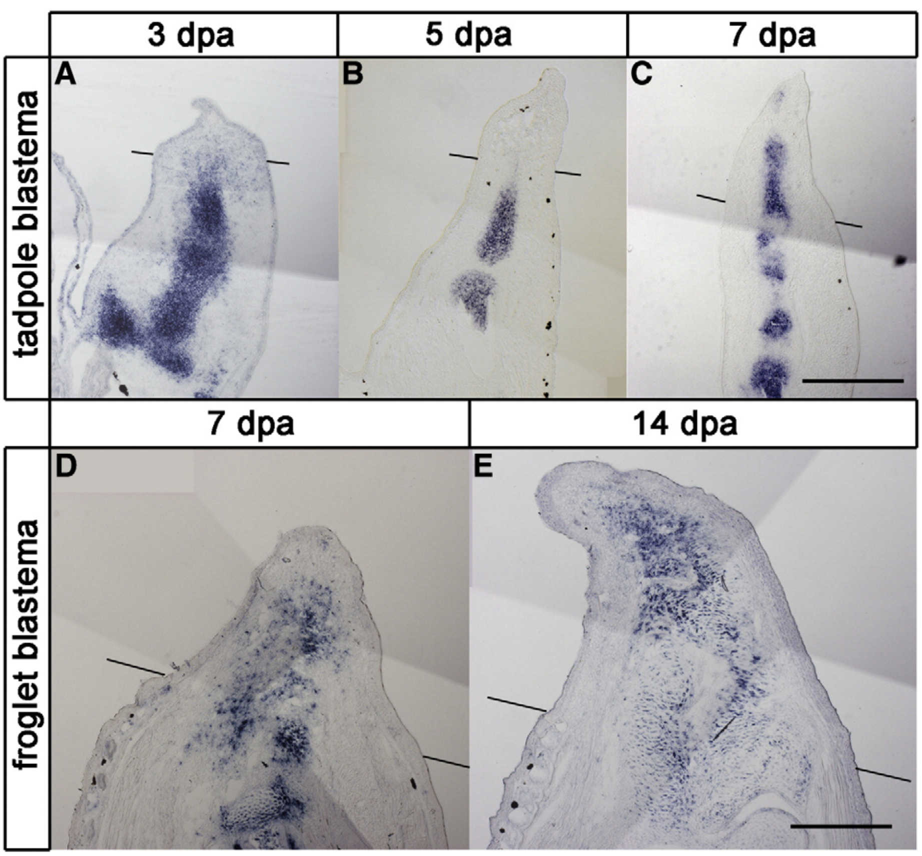

Fig. 4. Expression of cartilage maker gene, *sox9*, in tadpole and froglet blastemas. Limbs were amputated at the ankle level of tadpole hindlimb bud (A–C) or at the wrist level of froglet forelimb (D, E). (A) Expression in tadpole 3 days post amputation (dpa) blastema. Expression was observed in the proximal to amputation plane but not in the blastema. (B) Expression in tadpole 5 dpa blastema. Expression was observed in the proximal to amputation plane but not in the blastema. (C) Expression in tadpole 7 dpa blastema. Expression was observed distal and proximal to the amputation plane. (D) Expression in froglet 7 dpa blastema. Expression was observed in the blastema. (E) Expression in froglet 14 dpa blastema. Expression was observed in a broad region of the blastema. Lines indicate the estimated amputation planes. Distal is to the top in all figures. Scale bar = 400 μm.

when cells from the same position are combined, they will form uniform mixtures (Ide et al., 1994). Mesenchymal cells from *Xenopus* limb buds will also be sorted based on their positions along the PD axis (Koibuchi and Tochinai, 1998). To examine which downstream effectors were disrupted by the altered expression of *hoxa13* and *hoxa11* in the froglet blastema, we examined whether *Xenopus* blastema cells have position-dependent cell affinity properties.

Xenopus stage 53 hindlimb buds were divided into three equal regions along the PD axis (Fig. 5A), and cells from the first (Dis) and third (Pro) regions were mixed. When distal region cells were labeled with a fluorescent dye and mixed with unlabeled cells from the same distal region, the cultures showed uniform mixing of labeled and unlabeled cells (Fig. 5A, Dis vs. Dis). Labeled distal region cells and unlabeled proximal cells showed sorting, however (Fig. 5A, Dis vs. Pro). These results indicate that surfaces of *Xenopus* limb bud cells contain signals that indicate their position along the PD axis. Similar sorting was observed with blastema cells from different amputation levels at tadpole stage 53. We divided the blastema at the knee level into three PD parts. The distal region (Dis in Fig. 5B) has a *hoxa13*-single-positive condition similar to the ankle level blastema (DB), presumably giving rise to the autopod. The proximal region (Pro) has a *hoxa11*-single-positive condition that presumably gives rise to the zeugopod. We discarded the intermediate part (Int) between them. When labeled blastema cells derived from the ankle level (DB) were mixed with unlabeled distal region cells (Dis) from blastemas at the knee level (Fig. 5B), no or little sorting was observed (Fig. 5B, DB vs. Dis). When blastema cells at the ankle level (DB) and cells from the proximal region of blastemas (Pro) at the knee level were mixed, however, the cells displayed position-specific aggregation (Fig. 5B, DB vs. Pro). These results support the idea that tadpole blastema cells, like limb bud cells, show cell adhesion properties that are dependent on their positions along the PD axis. In particular, distal cells of blastemas at the knee level, which contribute to the distal regenerate (autopod region), seem to have the same property as those at the autopod level.

Next, we carried out similar experiments using froglet blastema cells, which will only regenerate a spike structure. We divided the froglet blastema at the elbow level into three parts corresponding to those in the tadpole blastemas (Compare Fig. 5C with Fig. 5B). When labeled blastema cells at the wrist level (DB in Fig. 5C) were mixed with unlabeled distal region cells (Dis) from blastemas at the elbow level, no or little segregation was observed (Fig. 5C, DB vs. Dis). Interestingly, when cells from blastemas at the wrist level were mixed with cells from the proximal region of blastemas (Pro) at the elbow level, no or little segregation was again observed (Fig. 5C, DB vs. Pro). Thus, froglet blastema cells may not have differential cell surface properties along the PD axis.

EphA4 expression in the froglet blastema

In the chick limb system, anti-EphA4 antibodies have been used to abolish cell sorting along the PD axis, and overexpression of *ephrin-A2* was shown to modulate the affinities of mesenchymal cells that

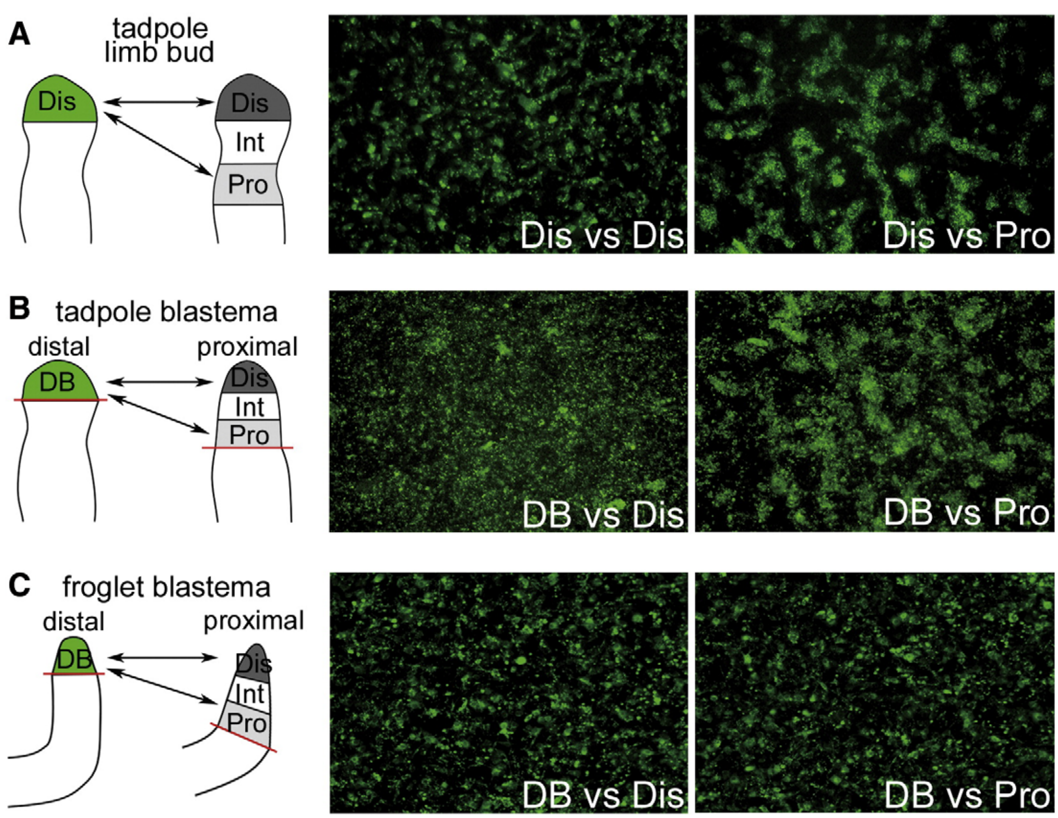

Fig. 5. Differential cell adhesiveness along the proximal–distal axis. (A) Cell sorting assay in the tadpole limb bud. Limb buds at stage 53 were divided into three (proximal, intermediate and distal) regions of equal length along the PD axis. When labeled distal region (Dis) and non-labeled distal regions (Dis) were mixed, sorting out was never observed (Dis vs. Dis). When labeled distal region (Dis) and non-labeled proximal regions (Pro) were mixed, sorting out was observed (Dis vs. Pro). (B) Cell sorting assay in the tadpole blastema. 7 days post amputation (dpa) blastemas from proximal (knee) level amputation (right) were divided into three (proximal, intermediate and distal) regions of equal length along the PD axis. When labeled 5 dpa distal (ankle level amputation) blastemas (DB) and non-labeled distal region of blastema derived from amputation at the proximal level (Dis) were mixed, sorting out was never observed (DB vs. Dis). When labeled 5 dpa distal blastemas (DB) and non-labeled proximal region of blastema derived from amputation at the proximal level (Pro) were mixed, sorting out was observed (DB vs. Pro). (C) Cell sorting assay in the froglet blastema. 14 dpa blastemas from proximal (elbow) level amputation (right) were divided into three (proximal, intermediate and distal) regions of equal length along the PD axis. When labeled 14 dpa blastemas from distal (wrist level amputation) level amputation (DB) and non-labeled distal region of blastema derived from amputation at the proximal level (Dis) were mixed, sorting out was never observed (DB vs. Dis). When labeled 14 dpa blastemas from distal level amputation (DB) and non-labeled proximal region of blastema derived from amputation at the proximal level (Pro) were mixed, sorting out was never observed (DB vs. Pro). Red bar indicates amputation plane. Black area in the pictures is filled with unlabeled cells.

differentiate into autopod elements (Wada et al., 1998, 2003). These results strongly suggest that ephrinA (ligand) and EphA (receptor tyrosine kinase expressed in the distal limb bud) are involved in cell sorting along the limb PD axis (Wada et al., 2003).

These results together with studies showing that *hoxa13* regulates cell surface properties (Yokouchi et al. 1995; Stadler et al. 2001) led us to analyze ephrinA/EphA signaling in the regenerating blastema. We found that *EphA4* was expressed in mesenchymal cells at the distal limb bud during *Xenopus* hindlimb development (stage 53, Fig. 6A). The expression of *EphA4* was also reactivated 3 dpa in the tadpole blastema at the ankle level (Fig. 6B). The *EphA4*-expressing domain was shifted distally and was restricted to the distal blastema at 5 dpa (Fig. 6C). This distal expression domain resembles that of *hoxa13* in the tadpole blastema (compare Fig. 6C with Fig. 2F). In contrast to the tadpole blastema, we did not detect *EphA4* expression in the froglet limb blastema. At 7 dpa and 14 dpa, no signal was detected with an *EphA4*-specific probe although nonspecific staining was observed in secretory glands (Figs. 6D and E).

Quantitative analysis of hoxa11 and hoxa13 expression

In a previous *in vitro* study, limb mesenchymal cells from a *hoxa13* mutant mouse did not sort based on their positions along the PD axis (Stadler et al., 2001), and *hoxa13* misexpression has suggested that the protein product regulates the position-specific signals along the PD axis (Yokouchi et al., 1995). We hypothesized that the *hoxa13* expression level in the froglet blastema was low compared with that in the tadpole blastema and that this lower expression level disrupted cell sorting, resulting in the patternless phenotype. To assess this hypothesis, we examined the expression levels of *hoxa11*, *hoxa13*, and *sox9* in blastemas at the ankle or wrist level using real-time RT-PCR analysis. *hoxa11* expression levels were higher in froglet 14 dpa blastemas and no significant difference was observed between froglet later stage blastemas and tadpole 7 dpa blastemas (Fig. 7A). *hoxa13* expression was also weak in froglet 7 dpa blastemas compared with that in tadpole blastemas, although the expression levels increased in froglet 14 dpa blastemas (Fig. 7B). *hoxa13* expression levels, however, were significantly lower in froglet blastemas than in tadpole blastemas. These results indicate that although the re-expression of *hoxa13* was detectable, *hoxa13* mRNA levels were relatively low. *sox9* expression in froglet blastemas was more robust compared with tadpole blastemas (Fig. 7C), while the expression domains of *hoxa11* and *hoxa13* did not separate (Figs. 3E, F). This observation of chondrogenesis (*sox9* expression) prior to the completion of pattern formation (separation of the *hoxa11* and *hoxa13* expression domains) was consistent with our *in situ* hybridization results (Fig. 4).

Discussion

Differences in HoxA gene expression during limb development and regeneration in regenerative and nonregenerative limbs

As shown in Fig. 1, a nested expression pattern of the Abdominal-B type genes *hoxa11* and *hoxa13* was observed in the early *Xenopus* limb bud. These expression domains then subsequently separated along the PD axis. Thus, the expression of *hoxa11* of *hoxa13* in the developing *Xenopus* limb bud is consistent with results from previous studies (Blanco et al., 1998; Endo et al., 2000; Lombardo and Slack, 2001). Furthermore, the temporal change in expression domains was similar to that reported in amniotes (Yokouchi et al., 1991; Nelson et al., 1996; Yashiro et al., 2004), suggesting that *hoxa11* and *hoxa13* functions during PD axis patterning are conserved among tetrapods. Importantly, in teleost pectoral fin buds, both *hoxa11* and *hoxa13* can be detected distally, but the overlapping domains do not completely separate along

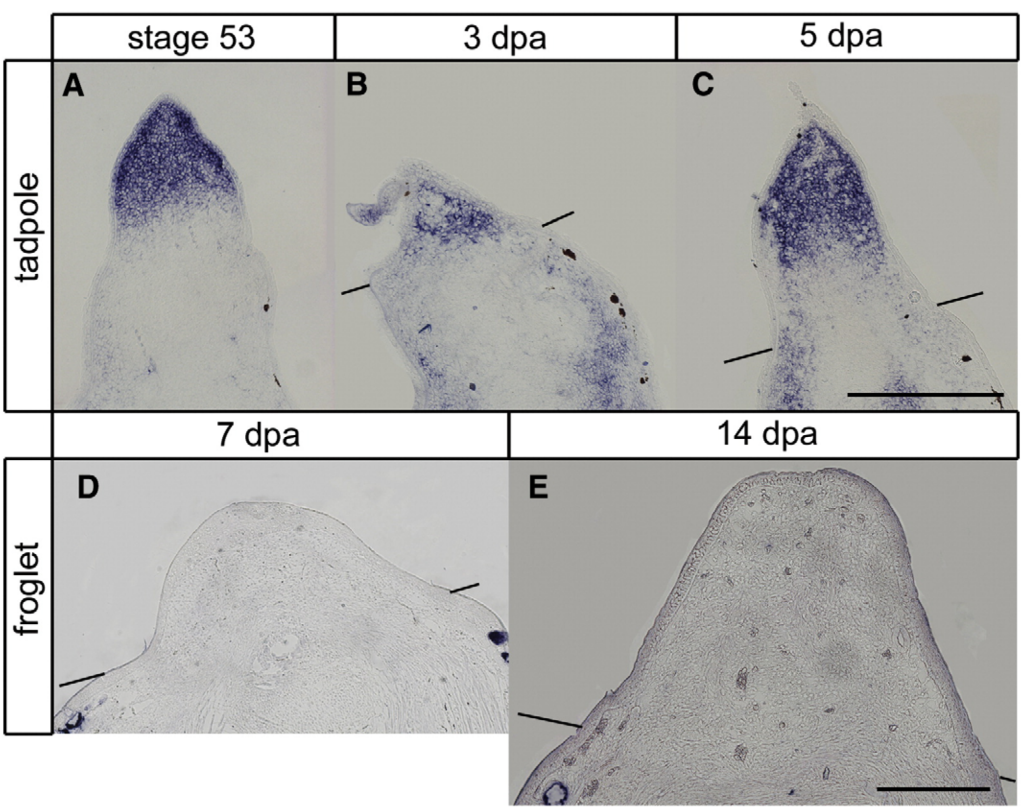

Fig. 6. Expression of *EphA4* in limb bud and tadpole and froglet blastemas. Blastemas were derived from the ankle level of tadpole hindlimb bud (B, C) or at the wrist level of froglet forelimb (D, E). (A) Expression in stage 53 limb bud. (B) Expression in tadpole 3 dpa blastema. (C) Expression in tadpole 5 dpa blastema. (D) Expression in froglet 7 dpa blastema. (E) Expression in froglet 14 dpa blastema. Note that expression is not observed in the froglet blastema. Lines indicate the estimated amputation planes. Distal is to the top in all figures. Scale bar = 400 µm.

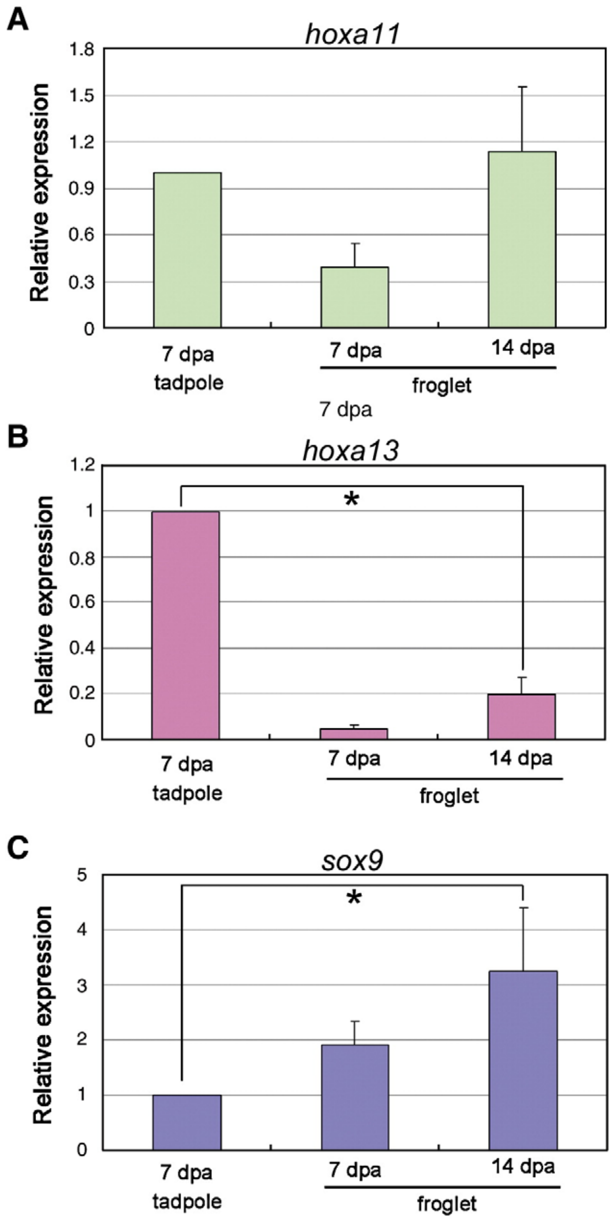

Fig. 7. Quantitative analysis of *hoxa11* (A), *hoxa13* (B) and *sox9* (C) gene expression levels in tadpole and froglet blastemas. Each gene expression level was measured by real-time RT-PCR using specific primers. The results were firstly normalized to ribosomal L8 and then represented as values relative to the expression levels in tadpole 7 dpa blastemas. Values represent the means of three independent experiments. Error bars indicate standard deviations. Data were analyzed by Welch's test, and differences were found to be statistically significant (*$P<0.05$).

the PD axis (Sordino et al., 1996; Neumann et al., 1999). The origin of autopods during vertebrate evolution and the causative molecular mechanisms have been the subject of much debate. Developing fin buds in such basal actinopterygians as *Polyodon spathula* show incomplete separation of the *hoxa11* and *hoxa13* expression domains (Metscher et al., 2005). Although the expression of *HoxA* genes in the fins of living sarcopterygians, such as lung fish, have not been reported, fossils records with incomplete autopods in the distal pectoral fins (Shubin et al., 2006; Boisvert et al., 2008) suggest successive steps in the transition from fins to limbs. Our observations confirm that PD axis formation, including the dynamic *hoxa11* and *hoxa13* expression profiles, is conserved among living tetrapods, suggesting a close relationship between the origin of autopods and the roles of *hoxa11* and *hoxa13* during PD axis formation.

Previous studies of anuran tadpoles and urodeles, both of which are able to regenerate their limbs, showed that at least 24 of 39 *Hox* genes were expressed in the blastema (reviewed by Gardiner and Bryant 2007). Although *hoxa11* and *hoxa13* expression was observed (Beauchemin et al., 1994; Gardiner et al., 1995; Christen et al., 2003), the spatial expression pattern of *hoxa11* was not examined during limb regeneration. According to our data, in the early stage tadpole blastema, *hoxa11* is expressed even when the limb bud is amputated at the ankle level (i.e., the zeugopod–autopod boundary). In the autopod region (i.e., distal to the ankle) of a developing *Xenopus* limb bud at stage 52, *hoxa13* is expressed strongly, whereas the expression of *hoxa11* was hardly detected (Fig. 1C, D). After ankle level amputation at stage 53, however, blastema cells express *hoxa11* in a broad area, and its expression domain overlaps with that of *hoxa13* (Fig. 2A). Then, the expression of *hoxa11* was no longer observed in the distal blastema (Figs. 2E, I). Although it is possible that the source of blastema cells at the wrist level is already *hoxa11*-positive and that the *hoxa11*-positive blastema cells begins to form the autopod, this appearance and cessation of *hoxa11* expression in the autopod blastema is interesting, because *hoxa11* itself is not essential for the autopod structure (Davis et al., 1995). During limb regeneration in axolotls, early blastema cells were suggested to have a distal identity because *hoxa9* and *hoxa13* are expressed synchronously, similar to the distal limb bud (Gardiner et al., 1995). The expression patterns of *hoxa11* and *hoxa13* during tadpole regeneration are consistent with this hypothesis. Alternatively, *hoxa11* expression may be initiated before *hoxa13* expression in the earlier blastema, which we could not detect in our experiments. We therefore do not exclude the possibility that the early process of PD patterning in limb regeneration recapitulates the developmental process, and the nested pattern of *hoxa11*/*hoxa13* supports this idea. Because of the genomic structure of these genes, re-expression of 3′ *Hox* genes, such as *hoxa11*, may be necessary to activate more 5′ Hox genes, including *hoxa13*. To address this hypothesis, it would be interesting to investigate the precise expression patterns and chromatin states of various *Hox* genes. The overlapping expression of *hoxa11* and *hoxa13*, however, may simply reflect that stump cells, which express *hoxa11*, supply the blastemas. To address this possibility, it is necessary to investigate *hoxa11* expression after amputation at the hand level, in which *hoxa11* is not expressed.

Compared with tadpole blastemas, froglet limb blastemas showed different *hoxa11* and *hoxa13* expression profiles during regeneration. In early stage blastemas, *hoxa11* and *hoxa13* expression domains clearly overlapped (Figs. 3A–D), suggesting that froglet blastemas begin to carry out at least early PD axis formation. Previous studies showed that froglet blastemas have some epimorphic characteristics that are similar to those of early stage urodele blastemas—e.g., vigorous cell proliferation, gene expression indicating an undifferentiated state, and a dependence on nerve activity (Endo et al., 2000; Suzuki et al., 2005, 2007). Reactivation of *hoxa11* and *hoxa13* expression indicates that these properties may also include the initiation of PD axis formation. However, the nested pattern of *hoxa11* and *hoxa13* expression was not obvious, *hoxa11* is expressed in the distal region of the froglet blastema, and the *hoxa11* and *hoxa13* expression domains did not separate along the PD axis. These results suggest that PD axis formation during froglet limb regeneration is disrupted. Cells that express either *hoxa11* or *hoxa13* may be mixed in the same blastema, or the blastema cells may still express both *hoxa11* and *hoxa13*. The cell sorting assays supports the latter possibility in the froglet blastema. Thus, the change in *HoxA* gene expression from *hoxa11*/*hoxa13* double-positive to *hoxa11* or *hoxa13* single-positive may not occur. These data together with our previous results suggesting that AP pattern formation and DV pattern formation do not occur appropriately in regenerating froglets (Endo et al., 1997; Matsuda et al., 2001; Yakushiji et al., 2007) demonstrate deficient pattern formation along all three axes. Whether these defects are interrelated remains unknown, and further investigations are required to show whether rescuing one axis also allows proper patterning along the other axes.

Potential contributions of hoxa11 and hoxa13 expression to defective patterning

Chick limb bud cells exhibit different cell affinity properties along the PD axis, which is important for PD pattern formation (Ide et al., 1994; Wada et al., 1998; Sato-Maeda and Ide, 1998). We have shown the presence of different cell affinities along the PD axis in *Xenopus* tadpole limb buds (Fig. 5A Dis vs. Dis, Dis vs. Pro). Furthermore, *Xenopus* tadpole blastema cells from different positions along the PD axis sorted in our assay (Fig. 5B DB vs. Dis, DB vs. Pro), suggesting that pattern-regenerating blastema cells also have position-dependent cell affinities. This is supported by the results from an *in vivo* assay showing that the adhesive properties of axolotl blastema cells form a gradient along the PD axis (Nardi and Stocum, 1983).

Although both limb bud and blastema cells at the tadpole stage have position-dependent cell affinities, froglet blastema cells did not display this property (Fig. 5C DB vs. Dis, DB vs. Pro). This indicates that defects in PD patterning during froglet limb regeneration are mediated by altered cell surface properties. We propose that the cell surfaces of blastema mesenchymal cells in the froglet blastema are homogeneous, and do not display PD positional information. This may result in the formation of spike structures wherever the froglet limb is amputated.

Our results also revealed an absence of *EphA4* expression in the froglet blastema (Figs. 6D, E), which correlates with the lack of cell sorting. ephrin/Eph signaling is known to be involved in the sorting of limb mesenchymal cells along the PD axis and limb patterning (Wada et al., 1998, 2003). In *hoxa13* mutant mice, for example, *EphA7* expression is markedly reduced and the mutant mesenchyme cells in the future autopod region fail to sort normally, resulting in impaired autopod formation (Stadler et al., 2001). Interestingly, Eph receptors are direct downstream targets of *hoxa13* in the developing limb (Salsi and Zappavigna, 2006). These results support the idea that *hoxa13* regulates cell surface properties via ephrin/Eph signaling. We demonstrated that the *hoxa11* and *hoxa13* expression domains never separated and that *hoxa13* mRNA levels were low in the froglet blastema (Figs. 3 and 7B). Thus, downregulation of *hoxa13* expression may disrupt ephrin/Eph signaling, which in turn prevents cell sorting and PD pattern formation.

Possible causes of altered hoxa11 and hoxa13 expression

Several possibilities may have resulted in the differences in the *hoxa11* and *hoxa13* expression patterns. For instance, changes in the signaling cascades upstream of the *HoxA* genes, such as the retinoic acid (RA) pathway, may disrupt PD patterning. RA is involved in PD patterning during both limb development and regeneration (Maden, 1982; Crawford and Stocum, 1988; Tamura et al., 1997; Maden and Hind, 2003; Yashiro et al., 2004). *cyp26b1*, which encodes a cytochrome P450 enzyme that inactivates RA, is expressed in the distal region of the developing limb bud (MacLean et al., 2001); mice lacking this gene show RA-related signaling in the distal end of the developing limb and PD pattern defects (Yashiro et al., 2004). Furthermore, excess levels of RA proximalized distal blastemas during urodele limb regeneration, and the degree of proximalization increased with the RA dose (Maden, 1982; Crawford and Stocum, 1988). It is possible that changes in the RA gradient in *Xenopus* froglet blastemas have resulted in defective PD patterning. RA concentrations in *Xenopus* blastemas have been measured along the AP axis, which did not show a RA gradient (Scadding and Maden, 1994), whereas RA concentrations along the PD axis have not been examined. Future studies may also investigate the expression of RA related metabolic enzymes and differences in RA activity along the PD axis in both tadpole and froglet blastemas.

A second possibility is that a shift in the timing between pattern formation (i.e., separated *hoxa11* and *hoxa13* expression domains) and cell differentiation (i.e., chondrogenesis) causes aberrant PD patterning. In the tadpole developing limb bud and regenerating blastema, pattern formation along the PD axis is followed by cell differentiation. In the froglet blastema, differentiation of the cells into chondrocytes begins before PD patterning is complete (compare Figs. 3 and 4). Prematured chondrogenesis may disturb PD patterning. Axolotl and newt limbs regenerate all of the tissue types, including cartilage and muscle, whereas the froglet stump develops into a cartilage-rich structure that lacks muscle tissue (Korneluk and Liversage, 1984; Satoh et al., 2005a). Thus, enhanced cartilage differentiation in the froglet blastema may perturb PD patterning, resulting in a patternless spike.

A third possibility is altered epigenetic regulation of gene expression. In the ef1-α:EGFP transgenic zebrafish line, in which EGFP is ubiquitously expressed in the embryo, the transgene is highly methylated and inactive in the adult caudal fin (Thummel et al., 2006). Interestingly, the transgene is demethylated and reactivated in the regenerating caudal fin blastema. These observations suggest that the complete regeneration of the zebrafish fin requires epigenetic control of gene expression, and in particular DNA demethylation-mediated transcriptional reactivation. On the other hand, the *Xenopus* froglet limb blastema does not express *shh* and the *shh* gene is highly methylated in the limb-specific enhancer region. This demonstrates that the silenced *shh* gene is not reactivated in the froglet limb (Yakushiji et al., 2007; Yakushiji et al., 2009). *Hox* genes are also epigenetically regulated by Polycomb group (PcG) and Trithorax group (trxG) proteins, which modify chromatin to induce the repression and activation of *Hox* genes, respectively (Orlando, 2003; Simon and Tamkun, 2003). Altered epigenetic regulation, such as changes in PcG genes that negatively regulate *hoxa11* expression in the autopod region, may disrupt the dynamic profile of *HoxA* gene expression in the froglet blastema.

These hypotheses are not mutually exclusive, and multiple factors might contribute to the limited regenerative ability of *Xenopus* froglet limbs. Investigations into this limited regenerative ability should lead to a better understanding of differences between regenerative and nonregenerative limbs. Our results provide evidence that defective PD patterning is a major reason that froglet limbs cannot regenerate. Further studies examining these three possibilities may elucidate methods to rescue pattern formation not only in *Xenopus* froglet limbs but also in nonregenerative limbs in other vertebrates, as well as the mechanisms governing pattern formation during organogenesis and organ regeneration.

Acknowledgments

We are grateful to Drs. Hiroyuki Ide, Kosei Sato, Gembu Abe and Hiroaki Yamamoto for helpful comments and discussion. We also thank Ellen Chernoff for critical reading of the manuscript and valuable comments. This work was supported by research grants from the Ministry of Education, Science, Sports and Culture of Japan, KAKENHI (Grant-in-Aid for Scientific Research) on Priority Areas "Comparative Genomics," and Toray Science Foundation.

References

Beauchemin, M., Noiseux, N., Tremblay, M., Savard, P., 1994. Expression of Hox A11 in the limb and the regeneration blastema of adult newt. Int. J. Dev. Biol. 38, 641–649.
Blanco, M.J., Misof, B.Y., Wagner, G.P., 1998. Heterochronic differences of Hoxa-11 expression in Xenopus fore- and hind limb development: evidence for lower limb identity of the anuran ankle bones. Dev. Genes Evol. 208, 175–187.
Boisvert, C.A., Mark-Kurik, E., Ahlberg, P.E., 2008. The pectoral fin of Panderichthys and the origin of digits. Nature 456, 636–638.
Capdevila, J., Izpisua Belmonte, J.C., 2001. Patterning mechanisms controlling vertebrate limb development. Annu. Rev. Cell. Dev. Biol. 17, 87–132.
Christen, B., Beck, C.W., Lombardo, A., Slack, J.M., 2003. Regeneration-specific expression pattern of three posterior Hox genes. Dev. Dyn. 226, 349–355.
Crawford, K., Stocum, D.L., 1988. Retinoic acid coordinately proximalizes regenerate pattern and blastema differential affinity in axolotl limbs. Development 102, 687–698.
Davis, A.P., Witte, D.P., Hsieh-Li, H.M., Potter, S.S., Capecchi, M.R., 1995. Absence of radius and ulna in mice lacking hoxa-11 and hoxd-11. Nature 375, 791–795.

Dent, J.N., 1962. Limb regeneration in larvae and metamorphosing individuals of the South African clawed toad. J. Morphol. 110, 61–77.

Endo, T., Yokoyama, H., Tamura, K., Ide, H., 1997. Shh expression in developing and regenerating limb buds of *Xenopus laevis*. Dev. Dyn. 209, 227–232.

Endo, T., Tamura, K., Ide, H., 2000. Analysis of gene expressions during Xenopus forelimb regeneration. Dev. Biol. 220, 296–306.

Gardiner, D.M., Blumberg, B., Komine, Y., Bryant, S.V., 1995. Regulation of HoxA expression in developing and regenerating axolotl limbs. Development 121, 1731–1741.

Gardiner, D.M., Bryant, S.V., 2007. Homeobox-containing genes in limb regeneration. In: Papageorgiou, S. (Ed.), HOX Gene Expression. Landes Bioscience and Springer, Texas, pp. 102–110.

Ide, H., Wada, N., Uchiyama, K., 1994. Sorting out of cells from different parts and stages of the chick limb bud. Dev. Biol. 162, 71–76.

Ide, H., Yokoyama, H., Endo, T., Omi, M., Tamura, K., Wada, N., 1998. Pattern formation in dissociated limb bud mesenchyme *in vitro* and *in vivo*. Wound Repair Regen 6, 398–402.

Iimura, T., Pourquie, O., 2007. Hox genes in time and space during vertebrate body formation. Dev. Growth Differ. 49, 265–275.

Imokawa, Y., Yoshizato, K., 1997. Expression of Sonic hedgehog gene in regenerating newt limb blastemas recapitulates that in developing limb buds. Proc. Natl. Acad. Sci. U. S. A. 94, 9159–9164.

Koibuchi, N., Tochinai, S., 1998. Existence of gradient in cell adhesiveness along the developing Xenopus hind limb bud, shown by a cellular sorting-out experiment in vitro. Dev. Growth Differ. 40, 355–362.

Korneluk, R.G., Liversage, R.A., 1984. Effects of radius—ulna removal on forelimb regeneration in *Xenopus laevis* froglets. J. Embryol. Exp. Morphol. 82, 9–24.

Lombardo, A., Slack, J.M., 2001. Abdominal B-type Hox gene expression in *Xenopus laevis*. Mech. Dev. 106, 191–195.

MacLean, G., Abu-Abed, S., Dollé, P., Tahayato, A., Chambon, P., Petkovich, M., 2001. Cloning of a novel retinoic-acid metabolizing cytochrome P450, Cyp26B1, and comparative expression analysis with Cyp26A1 during early murine development. Mech. Dev. 107, 195–201.

Maden, M., 1982. Vitamin A and pattern formation in the regenerating limb. Nature 295, 672–675.

Maden, M., Hind, M., 2003. Retinoic acid, a regeneration-inducing molecule. Dev. Dyn. 226, 237–244.

Matsuda, H., Yokoyama, H., Endo, T., Tamura, K., Ide, H., 2001. An epidermal signal regulates Lmx-1 expression and dorsal–ventral pattern during Xenopus limb regeneration. Dev. Biol. 229, 351–362.

Metscher, B.D., Takahashi, K., Crow, K., Amemiya, C., Nonaka, D.F., Wagner, G.P., 2005. Expression of Hoxa-11 and Hoxa-13 in the pectoral fin of a basal ray-finned fish, *Polyodon spathula*: implications for the origin of tetrapod limbs. Evol. Dev. 7, 186–195.

Muneoka, K., Holler-Dinsmore, G., Bryant, S.V., 1986. Intrinsic control of regenerative loss in *Xenopus laevis* limbs. J. Exp. Zool. 240, 47–54.

Nardi, J.B., Stocum, D.L., 1983. Surface properties of regenerating limb cells: Evidence for gradation along the proximodistal axis. Differentiation 25, 27–31.

Nelson, C.E., Morgan, B.A., Burke, A.C., Laufer, E., DiMambro, E., Murtaugh, L.C., Gonzales, E., Tessarollo, L., Parada, L.F., Tabin, C., 1996. Analysis of Hox gene expression in the chick limb bud. Development 122, 1449–1466.

Neumann, C.J., Grandel, H., Gaffield, W., Schulte-Merker, S., Nüsslein-Volhard, C., 1999. Transient establishment of anteroposterior polarity in the zebrafish pectoral fin bud in the absence of sonic hedgehog activity. Development 126, 4817–4826.

Nieuwkoop, P.D., Faber, J., 1956. Normal table of *Xenopus laevis* (Daudin). North-Holland Publ. Comp., Amsterdam.

Orlando, V., 2003. Polycomb, epigenomes, and control of cell identity. Cell 112, 599–606.

Robinson, H., Allenby, K., 1974. The effect of nerve growth factor on hindlimb regeneration in *Xenopus laevis* froglets. J. Exp. Zool. 189, 215–226.

Salsi, V., Zappavigna, V., 2006. Hoxd13 and Hoxa13 directly control the expression of the EphA7 Ephrin tyrosine kinase receptor in developing limbs. J. Biol. Chem. 281, 1992–1999.

Sato, K., Koizumi, Y., Takahashi, M., Kuroiwa, A., Tamura, K., 2007. Specification of cell fate along the proximal–distal axis in the developing chick limb bud. Development 134, 1397–1406.

Sato-Maeda, M., Ide, H., 1998. Juxtaposition of two heterotypic monolayer cell cultures of chick limb buds. Dev. Growth Differ. 40, 403–411.

Satoh, A., Ide, H., Tamura, K., 2005a. Muscle formation in regenerating Xenopus froglet limb. Dev. Dyn. 233, 337–346.

Satoh, A., Suzuki, M., Amano, T., Tamura, K., Ide, H., 2005b. Joint development in *Xenopus laevis* and induction of segmentations in regenerating froglet limb (spike). Dev. Dyn. 233, 1444–1453.

Satoh, A., Endo, T., Abe, M., Yakushiji, N., Ohgo, S., Tamura, K., Ide, H., 2006. Characterization of Xenopus digits and regenerated limbs of the froglet. Dev. Dyn. 235, 3316–3326.

Scadding, S.R., Maden, M., 1994. Retinoic acid gradients during limb regeneration. Dev. Biol. 162, 608–617.

Shi, Y.B., Liang, V.C., 1994. Cloning and characterization of the ribosomal protein L8 gene from *Xenopus laevis*. Biochim. Biophys. Acta 1217, 227–228.

Shubin, N.H., Daeschler, E.B., Jenkins Jr, F.A., 2006. The pectoral fin of *Tiktaalik roseae* and the origin of the tetrapod limb. Nature 440, 764–771.

Simon, J.A., Tamkun, J.W., 2003. Programming off and on states in chromatin: mechanisms of Polycomb and trithorax group complexes. Curr. Opin. Genet. Dev. 12, 210–218.

Sordino, P., Duboule, D., Kondo, T., 1996. Zebrafish Hoxa and Evx-2 genes: cloning, developmental expression and implications for the functional evolution of posterior Hox genes. Mech. Dev. 59, 165–175.

Stadler, H.S., Higgins, K.M., Capecchi, M.R., 2001. Loss of Eph-receptor expression correlates with loss of cell adhesion and chondrogenic capacity in Hoxa13 mutant limbs. Development 128, 4177–4188.

Steinberg, M.S., 1970. Does differential adhesion govern self-assembly processes in histogenesis? Equilibrium configurations and the emergence of a hierarchy among populations of embryonic cells. J. Exp. Zool. 173, 395–433.

Suzuki, M., Satoh, A., Ide, H., Tamura, K., 2005. Nerve-dependent and -independent events in blastema formation during Xenopus froglet limb regeneration. Dev. Biol. 286, 361–375.

Suzuki, M., Yakushiji, N., Nakada, Y., Satoh, A., Ide, H., Tamura, K., 2006. Limb regeneration in *Xenopus laevis* froglet. Scientific World J. 6 (Suppl. 1), 26–37.

Suzuki, M., Satoh, A., Ide, H., Tamura, K., 2007. Transgenic Xenopus with prx1 limb enhancer reveals crucial contribution of MEK/ERK and PI3K/AKT pathways in blastema formation during limb regeneration. Dev. Biol. 304, 675–686.

Tabin, C., Wolpert, L., 2007. Rethinking the proximodistal axis of the vertebrate limb in the molecular era. Genes Dev. 21, 1433–1442.

Tamura, K., Yokouchi, Y., Kuroiwa, A., Ide, H., 1997. Retinoic acid changes the proximodistal developmental competence and affinity of distal cells in the developing chick limb bud. Dev. Biol. 188, 224–234.

Tamura, K., Yonei-Tamura, S., Yano, T., Yokoyama, H., Ide, H., 2008. The autopod: its formation during limb development. Dev. Growth Differ. 50 (Suppl. 1), S177–S187.

Tamura, K., Ohgo, S., and Yokoyama, H. in press. The limb blastema cell: a stem cell for morphological regeneration. Dev. Growth Differ. (Epub ahead of print).

Thummel, R., Burket, C.T., Hyde, D.R., 2006. Two different transgenes to study gene silencing and re-expression during zebrafish caudal fin and retinal regeneration. Scientific World Journal 6 (Suppl 1), 65–81.

Torok, M.A., Gardiner, D.M., Izpisua Belmonte, J.C., Bryant, S.V., 1999. Sonic hedgehog (shh) expression in developing and regenerating axolotl limbs. J. Exp. Zool. 284, 197–206.

Tschumi, P.A., 1957. The growth of the hindlimb bud of *Xenopus laevis* and its dependence upon the epidermis. J. Anat. 91, 149–173.

Wada, N., Ide, H., 1994. Sorting out of limb bud cells in monolayer culture. Int. J. Dev. Biol. 38, 351–356.

Wada, N., Kimura, I., Tanaka, H., Ide, H., Nohno, T., 1998. Glycosylphosphatidylinositol-anchored cell surface proteins regulate position-specific cell affinity in the limb bud. Dev. Biol. 202, 244–252.

Wada, N., Tanaka, H., Ide, H., Nohno, T., 2003. Ephrin-A2 regulates position-specific cell affinity and is involved in cartilage morphogenesis in the chick limb bud. Dev. Biol. 264, 550–563.

Yajima, H., Yonei-Tamura, S., Watanabe, N., Tamura, K., Ide, H., 1999. Role of N-cadherin in the sorting-out of mesenchymal cells and in the positional identity along the proximodistal axis of the chick limb bud. Dev. Dyn. 216, 274–284.

Yakushiji, N., Suzuki, M., Satoh, A., Sagai, T., Shiroishi, T., Kobayashi, H., Sasaki, H., Ide, H., Tamura, K., 2007. Correlation between Shh expression and DNA methylation status of the limb-specific Shh enhancer region during limb regeneration in amphibians. Dev. Biol. 312, 171–182.

Yakushiji, N., Yokoyama, H., Tamura, K., 2009. Repatterning in amphibian limb regeneration: A model for study of genetic and epigenetic control of organ regeneration. Semin Cell Dev Biol. 20, 565–574.

Yashiro, K., Zhao, X., Uehara, M., Yamashita, K., Nishijima, M., Nishino, J., Saijoh, Y., Sakai, Y., Hamada, H., 2004. Regulation of retinoic acid distribution is required for proximodistal patterning and outgrowth of the developing mouse limb. Dev. Cell. 6, 411–422.

Yokouchi, Y., Sasaki, H., Kuroiwa, A., 1991. Homeobox gene expression correlated with the bifurcation process of limb cartilage development. Nature 353, 443–445.

Yokouchi, Y., Nakazato, S., Yamamoto, M., Goto, Y., Kameda, T., Iba, H., Kuroiwa, A., 1995. Misexpression of Hoxa-13 induces cartilage homeotic transformation and changes cell adhesiveness in chick limb buds. Genes Dev. 9, 2509–2522.

Yokoyama, H., 2008. Initiation of limb regeneration: the critical steps for regenerative capacity. Dev. Growth Differ. 50, 13–22.

Yokoyama, H., Endo, T., Tamura, K., Yajima, H., Ide, H., 1998. Multiple digit formation in Xenopus limb bud recombinants. Dev. Biol. 196, 1–10.

Yokoyama, H., Tamura, K., Ide, H., 2002. Anteroposterior axis formation in Xenopus limb bud recombinants: a model of pattern formation during limb regeneration. Dev. Dyn. 225, 277–288.

Yoshida, N., Urase, K., Takahashi, J., Ishii, Y., Yasugi, S., 1996. Mucus-associated antigen in epithelial cells of the chicken digestive tract: developmental change in expression and implications for morphogenesis-function relationships. Dev. Growth Differ. 38, 185–192.